Nuclear Instruments and Methods in Physics Research B 331 (2014) 15–19

Contents lists available at ScienceDirect

Nuclear Instruments and Methods in Physics Research B

journal homepage: www.elsevier.com/locate/nimb

The LILIA (laser induced light ions acceleration) experiment at LNF

S. Agosteo [a], M.P. Anania [b], M. Caresana [a], G.A.P. Cirrone [c], C. De Martinis [d], D. Delle Side [e], A. Fazzi [a], G. Gatti [b], D. Giove [d], D. Giulietti [f], L.A. Gizzi [g], L. Labate [g], P. Londrillo [h], M. Maggiore [i], V. Nassisi [e,*], S. Sinigardi [h], A. Tramontana [c], F. Schillaci [c], V. Scuderi [c,j], G. Turchetti [h], V. Varoli [a], L. Velardi [e]

[a] Energy Department, Polytechnic of Milan and INFN, Milan, Italy
[b] INFN LNF Frascati, Frascati, Italy
[c] INFN LNS Catania, Catania, Italy
[d] Physics Department, University of Milan and INFN, Milan, Italy
[e] LEAS, University of Salento and INFN, Lecce, Italy
[f] Physics Department, University of Pisa and INFN, Pisa, Italy
[g] INO-CNR and INFN, Pisa, Italy
[h] Physics Department, University of Bologna and INFN, Bologna, Italy
[i] INFN LNL, Legnaro, Italy
[j] Institute of Physics of the ASCR, Prague, Czech Republic

ARTICLE INFO

Article history:
Received 30 September 2013
Received in revised form 5 December 2013
Available online 30 January 2014

Keywords:
Laser driven ion acceleration
Proton beams
Hadron therapy

ABSTRACT

Laser-matter interaction at relativistic intensities opens up new research fields in the particle acceleration and related secondary sources, with immediate applications in medical diagnostics, biophysics, material science, inertial confinement fusion, up to laboratory astrophysics. In particular laser-driven ion acceleration is very promising for hadron therapy once the ion energy will attain a few hundred MeV. The limited value of the energy up to now obtained for the accelerated ions is the drawback of such innovative technique to the real applications. LILIA (laser induced light ions acceleration) is an experiment now running at LNF (Frascati) with the goal of producing a real proton beam able to be driven for significant distances (50–75 cm) away from the interaction point and which will act as a source for further accelerating structure. In this paper the description of the experimental setup, the preliminary results of solid target irradiation and start to end simulation for a post-accelerated beam up to 60 MeV are given.

1. Introduction

The acceleration of protons with compact devices is an active research area since hadron therapy has proved to be more effective with respect to conventional radiotherapy for a variety of tumours. The breakdown phenomena limits the maximum electric field of a conventional RF accelerator to a few tens of MV/m and even though this limit might be overcome with ad hoc design, no conclusive results have been achieved up to now. A promising alternative is offered by the very high fields which a plasma can sustain. When a short, high intensity laser pulse hits a thin target, the medium is almost instantaneously ionized and the displacement of electrons creates electric fields which can reach 1 MV/μm. As a consequence, in a few tens of microns an energy of 60 MeV, which is the threshold of interest for the therapy, could be reached. This is one of the strong motivations for the research on laser acceleration which has been very active during the last decade [1–3] This proton energy has been first reached with longer pulses (~1 ps) whose power exceeds 0.5PW [4] and approached only recently with a laser pulse power below 0.5 PW and pulse duration of 40 fs [5]. The Ti:Sa lasers with pulse durations of 25 fs and power up to 1 PW are commercially available and have been installed in several laboratories worldwide. In Italy at the Frascati INFN national laboratory, the laser FLAME is available with a nominal peak power of 220 TW. Taking advantage of this facility, an experiment named LILIA (laser induced light ions acceleration) has been conceived as an initial experimental and theoretical activity in the field of proton acceleration. In the initial stage, the experimental setup has been designed and assembled and first experiments with thin metal targets to accelerate protons in the target normal sheath acceleration (TNSA) regime at low intensity 1–3 W/cm^2 has been carried out. The next step would be to increase the intensity up to 10^{21} W/cm^2 and to develop a transport line to select the beam in angle and energy, making it suitable for further use such as injection into a conventional high frequency RF linac. The final goal of LILIA is to obtain a beam whose quality is comparable with that obtained by a conventional accelerator in a stable and reproducible

* Corresponding author.
E-mail address: vincenzo.nassisi@le.infn.it (V. Nassisi).

0168-583X/$ - see front matter © 2014 Elsevier B.V. All rights reserved.
http://dx.doi.org/10.1016/j.nimb.2013.12.035

way. This is of crucial importance for the direct use of the beam or its injection into an accelerating structure.

2. Scaling laws and PIC simulations

Currently, the most stable and reliable acceleration mechanism is the so-called TNSA [6], which occurs when solid targets are used far from the transparency limit. The laser pulses we consider in our modeling are Gaussian with a longitudinal profile given by $f(z) = cos^2(\pi z/c\tau)$, while the time dependence is given by $f(z-ct)$ and τ is the pulse duration. As a consequence the transverse component of the electric field reads

$$E(r,z,t) = E_0 w_0 w^{-1}(z) \exp\left(-\frac{r^2}{w^2(z)} + i\Phi(r,z)\right) e^{ik_0(z-ct)} f(z-ct) \quad (1)$$

$$w(z) = w_0\left(1+\frac{z^2}{z_R^2}\right)^{\frac{1}{2}} \quad (2)$$

where w_0 is the transverse waist of the laser, $w(z)$ is the longitudinal profile, $Z_R = k_0 w_0^2/2$ is the Rayleigh length and $\phi(r,z) = \frac{zr^2}{z_R w^2(z)} - arctan\left(\frac{z}{z_R}\right)$ is the phase factor. This paraxial approximation is accurate as long as $\epsilon << 1$, where $\epsilon = w_0/z_R = \lambda_0/(\pi w_0)$, the error being of order ϵ^2. Usually the duration FWHM is considered as $\tau_{FWHM} = 0.364\tau$. The target we consider is a thin metal foil, that we assume to be instantly ionized by the laser. We consider also the possibility of having a preplasma created by the precursors of the main pulse. Its density is typically a function of the distance from the target, and is usually represented as an exponential ramp. The pulse penetrates for a short distance of the order of a skin depth and heats the electrons which diffuse creating an electrostatic field at the rear surface of the target. In the 1D case the Poisson–Vlasov equation can be solved and gives for the protons an exponential energy spectrum [7] with cut-off

$$\frac{dN}{dE} = \frac{N_0}{E_0} exp\left(-\frac{E}{E_0}\right) \; for \; E < E_{max} \quad \frac{dN}{dE} = 0 \; for \; E > E_{max} \quad (3)$$

where $E_0(MeV) \infty 0.5a$ is the average energy (with a being the dimensionless laser amplitude), $E_{max}(MeV) \infty 2a$ is the maximum energy and N_0 is the total number of protons. Experimental results and 3D simulations show that the ratio is higher, namely $E_{max}/E_0 \sim 8$, whereas the ratio obtained from 2D simulations is close to 6. The relation between the dimensionless vector potential a and the intensity is given by $a = 0.68 \times 10^{-9} I^{1/2}$ [W/cm^2] for a linearly polarized pulse with $\lambda_0 = 0.8$ μm typical of Ti:Sa lasers. The most recent experimental results [8] have given E_{max} slightly below 20 MeV for a pulse with a peak value $a = 22$ and $\tau_{FWHM} = 25$, whereas with a longer pulse $\tau_{FWHM} = 40$ fs and peak intensity corresponding to $a \sim 28$ the measured value of E_{max} was over 40 MeV [5]. The 2D simulations for bare metal target such as Al of thickness $\ell \sim 1$ μm with a thin layer of contaminants on the rear side give a scaling $E_{max} \sim 2a$, whereas the presence of a foam layer considerably increases the maximum energy as shown by Fig. 1. When the thickness is decreased, the rise of E_{max} with respect to a is faster than linear. This is due to a change of regime since the radiation pressure acceleration effect grows until induced transparency is reached for $\pi\sigma = a$ where $\sigma = \ell n/\lambda_0 n_c$ is the dimensionless areal density of the target, with n and n_c being respectively the plasma density and the corresponding critical density. The optimal thickness [9] is $\ell_{opt} = \lambda_0(3+0.4a)^{-1} n_c/n$ and for a realistic target with $\ell \sim \lambda_0 = 0.8$ μm it is about 30 nm. This empirical law was nicely confirmed by our 2D simulations, done with our Particle In Cell (PIC) ALaDyn code[10].

From some preliminary simulations, the effect of a preplasma seems similar to the one induced by a foam with quasi-critical density. Different profiles have been considered in our studies. Several 2D simulations for a bare target of thickness between 0.3 μm and 1 μm confirm that the scaling is $E_{max}(MeV) \sim 2a$, whereas for targets where a foam layer or a preplasma is present on the upstream layer $E_{max}(MeV) \sim 3a$. For the bare foil, in the same thickness range, 3D simulations results suggest $E_{max}(MeV) \sim 1.5a$. The maximum energy depends also on the incidence angle α and incidence at 45° allows at least 20% more energy to be gained with respect to normal incidence. Assuming this law for the experiment in Frascati with $I = 1-4 \times 10^{19}$ W/cm^2 we find E_{max} in a range from 3 to 6 MeV. As shown below, this value is compatible with our experimental observations.

A usable ion/proton beam must have a definite energy E with a small spread ΔE, a sufficient number of protons ΔN, a small angular spread and emittance. The generation of a monochromatic beam directly by the laser pulse is currently a challenge because of the large energy distribution and divergence: indeed with a suitable transport line one can select an energy slice of the desired spread ΔE. What really matters is the number of protons in this slice. The number ΔN of protons in the selected slice depends on the chosen energy E and its spread ΔE. Close to the maximum energy, the number of protons is very low. A reasonable compromise may be found at a value of energy of $E = E_{max}/2$.

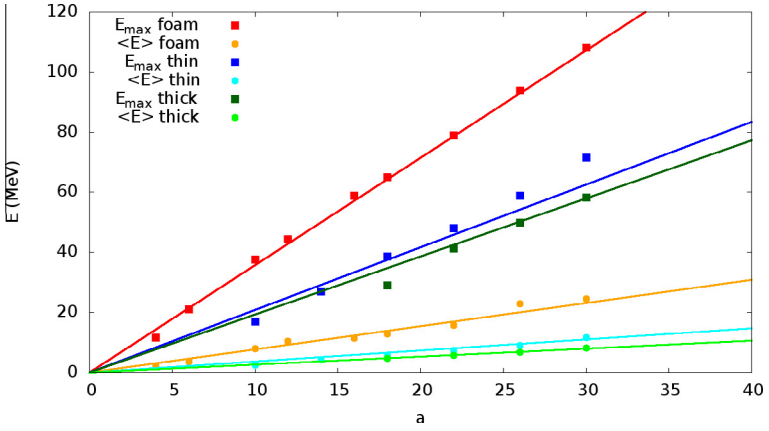

Fig. 1. PIC 2D parametric scan done with ALaDyn [10]. Variation with a of the maximum energy E_{max} and proton temperature E_0 for a laser pulse with $\tau_{FWHM} = 25$ fs. We compare a triple layer target (composed by a 2 μm H layer of foam, $n = 2n_c$, a 0.3 μm Al foil with $n = 60n_c$ and a 0.06 μm H layer of contaminants with $n = 9n_c$), representing with red squares the E_{max} and with orange circles E_0, with two double layer targets without foam of thicknesses 0.3 μm (blue squares E_{max}, cyan circles E_0) and 0.8 μm (dark green squares E_{max}, green circles E_0). (For interpretation of the references to color in this figure legend, the reader is referred to the web version of this article.)

Recent 3D PIC simulations with parameters close to the experiment described in [5] with $a = 30$ corresponding to a peak intensity $I = 2 \times 10^{21}$ W/cm^2 for a laser pulse duration of 40 fs have given a maximum energy of 55 MeV and an average energy $\langle E \rangle$ = 10 MeV. In that case it was proved that after an initial angle selection at 50 mrad and energy selection at 30 MeV with a solenoid, over 10^8 protons could be obtained with a rather narrow peak. After injection into a high field linac, the final number of 60 MeV protons was calculated to be close to 10^7 just at the threshold of interest for therapy.

3. The LILIA experiment

LILIA (*Laser Induced Light Ions Acceleration*) is an experiment of light ions acceleration trough laser interaction with thin metal targets to be done at the FLAME facility in Frascati. LILIA, in particular, is finalized to study, design and verify a scheme which foresees the production, the characterization and the transport of a proton beam toward a stage of post acceleration. The FLAME high power laser system has been recently fully commissioned [11]. It is based upon a Ti:Sa, chirped pulse amplification (CPA) laser able to deliver up to 220 TW laser pulses, 25 fs long, with a 10 Hz repetition rate at the fundamental wavelength of 800 nm. The system features a high contrast ratio (>10^{10}) and has a fully remotely controlled operation mode. In the typical current experimental conditions, the laser pulse is actually focused at peak intensities exceeding 10^{19} W/cm^2. In this configuration, according to the performed numerical simulations, we expect a proton beam with maximum energy of a few MeV and total intensities up to 10^{10}–10^{12} protons/shot. These values are modest compared to the present state of art for 100 TW class lasers, due to the currently used focusing optics (F/10). A reconfiguration of the focusing optics is already planned that will soon deliver a 5 times more intensity. An additional increase of up to a factor of 2 will come from the phase front correction. Ultimately, the focusing configuration for LILIA will use an F/2 focal length OA Parabola capable of giving a waist ≈2.5 μm with a corresponding intensity of $I \approx 10^{21}$ W/cm^2). In this case, we estimate that we might select a bunch at $E = 30$ MeV with a narrow spread ΔE of the order of 1% and still have a reasonable number of protons (10^7 – 10^8). This will open a very interesting perspective for applications such as hadron therapy in connection with a post-acceleration stage in order to reach energies up and beyond 100 MeV.

At this stage, attention was given to the initial tests and to the development of diagnostic techniques and to the laser-target optimization.

The LILIA experiment has been designed to be housed in the interaction chamber available at the exit of the laser compressor in the FLAME target area. The layout of the first phase of the experiment is shown in Fig. 2.

Preliminary tests with the beam on target have been recently carried out. During these tests energy was limited to approximately 2 J giving a laser intensity on target just below 10^{19} W/cm^2. Nevertheless we have obtained the first experimental evidence of proton acceleration.

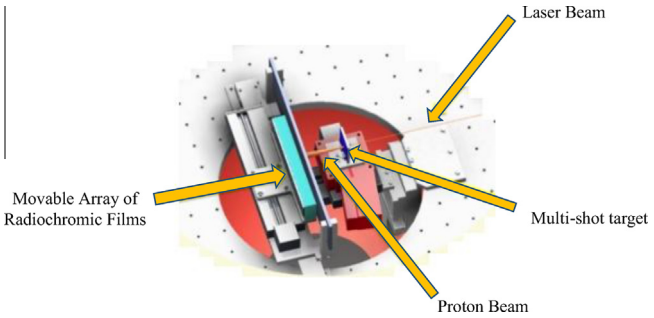

Fig. 2. Sketch of the LILIA mechanical setup.

The EBT3 radiochromic detectors were arranged in a stack of 5 elements and each one has been modified removing the front polyester layer of 120 microns. In this way, the protons could interact directly with the sensitive material of the first detector and all the other 4 sensitive layers are separated only by the remaining 120 micron polyester layer. This makes the stack more sensitive to low energy particles. Moreover the stack was shielded by a 6 μm thick aluminum foil in order to protect it from the laser and other optical emission during the laser interaction.

Fig. 3 shows the pictures of an EBT3 stack impressed by protons emitted from a 3 μm Al target with a 1.5 J laser shot. We may see that the emitted protons have impressed only the first element.

Using the proton range–energy correlation [12] we can derive a lower limit for the maximum energy of the emitted protons of at least 1.6 MeV. This energy value is related to a number of protons which release at least a dose of few cGy, being this the sensitivity threshold of the radio-chromic films used. This result is confirmed by measurements performed using CR39 instead of radiochromic films, in the same experimental conditions. Fig. 4 shows different pictures of the impressed CR39, taken at 0.5 mm steps from the centre of the interaction.

The core of the proton-CR39 interaction is saturated and the only information we can derive is given by the range-energy relation. Nevertheless far from the saturated region we can observe the presence of single resolved tracks. The microscopic analysis of these tracks after etching gives information on the particle species and their energy, resulting in the spectral distribution of Fig. 5, which extends up to 5 MeV. These energetic protons, considering the distance target-detector and the emission angle are most likely scattered on the target holder.

We plan in the near future to perform a parametric study of the correlation of the maximum TNSA accelerated proton energy, with respect to the following parameters:

- Laser pulse intensity (in the range 10^{18}–5 10^{19} W/cm^2).
- Laser pulse energy (in the range 0.1–5 J).
- Laser pulse length (in the range 25 fs – 1 ps).
- Metallic target thickness (in the range 1–3 μ).

Fig. 3. Impressed EBT3 radio-chromic film.

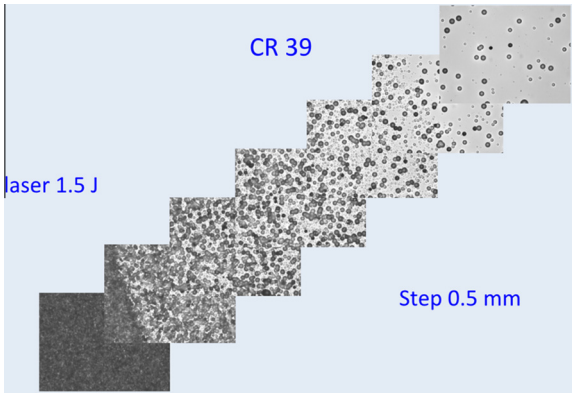

Fig. 4. Pictures of the impressed CR-39 taken from the same frame at steps of 0.5 mm. The CR39 film, also shielded to stop debris, shows a damaged black region in correspondence of the collimated emitted particles and the evidence of scattered protons in the surrounding area.

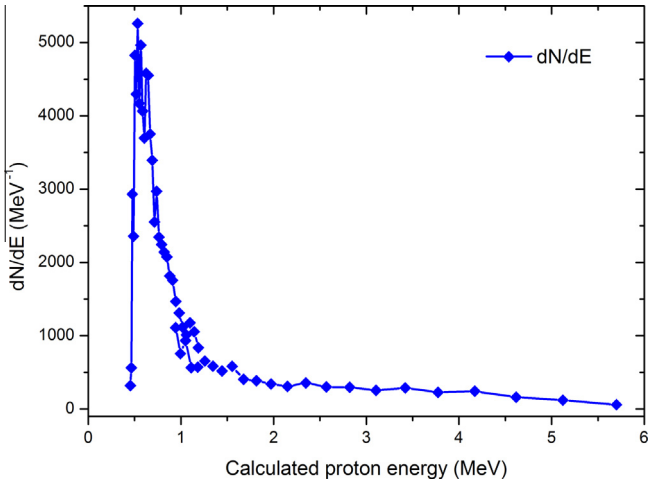

Fig. 5. Proton energy spectra as derived from the CR39 analysis.

3. Beam focusing and transport

The problem to immediate focus the emitted protons in order to obtain a useful beam and to transport it from the interaction region toward external measurement area or post-acceleration facilities, has been faced both from numerical computation and experimental point of view. The inherent large divergence and the energy spread can make it hard to utilize the full flux of the proton beam for applications and indeed for further transport and beam manipulation. The possibility to drive a laser emitted proton beam using a scheme based on a pulsed solenoid has been reported in literature [13]. We considered this approach really interesting and we carried out very preliminary simulation runs to define the main features of the components involved. At the same time, we have started an experimental program for the development of high field solenoid fed by a pulsed power supply in order to minimize thermal dissipation.

In view of the second phase initially proposed for the LILIA experiment, we have developed start-to-end simulations of laser acceleration and transport for two slightly different pulses with $a = 30$ and $\tau_{FWHM} = 30$ fs and 40 fs, respectively and Al target of thickness $\ell = 0.3$ μm and 0.8 μm, respectively and density $n = 60n_c$ [14,15]. In both cases there is a low density layer $(n \sim 2n_c)$ of thickness 2 μm on the upstream side. The contaminants layer on the downstream side has $n = 9n_c$ and thickness 0.06 μm. For the focusing a solenoid with peak magnetic field $B = 10$ T was considered in both cases: 4 cm aperture allows to capture all the beam after selection at $\theta < 50$ mrad. A second collimator placed on the focus of the lens for the selected energy allows to obtain a strongly peaked final spectrum. In Fig. 6 we show the final energy spectrum with selection energy at 30 MeV where over 10^8 protons are present in a window of 1 MeV. As a booster accelerator we have considered the use of a compact linear accelerator as the ACLIP one (Linear Compact Accelerator for Protontherapy)

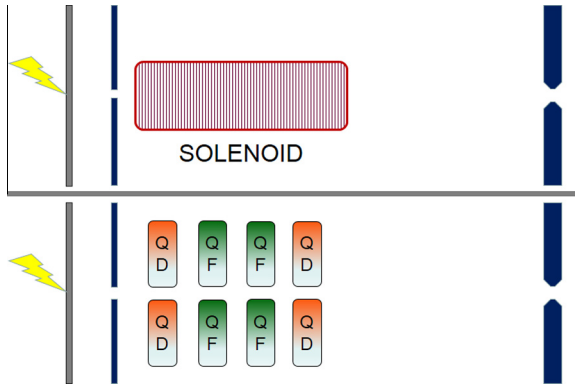

Fig. 7. Top: transport line with one solenoid and two collimators, the first one for angle selection and the second one for energy selection. Bottom: transport line with four permanent magnetic quadrupoles and two collimators.

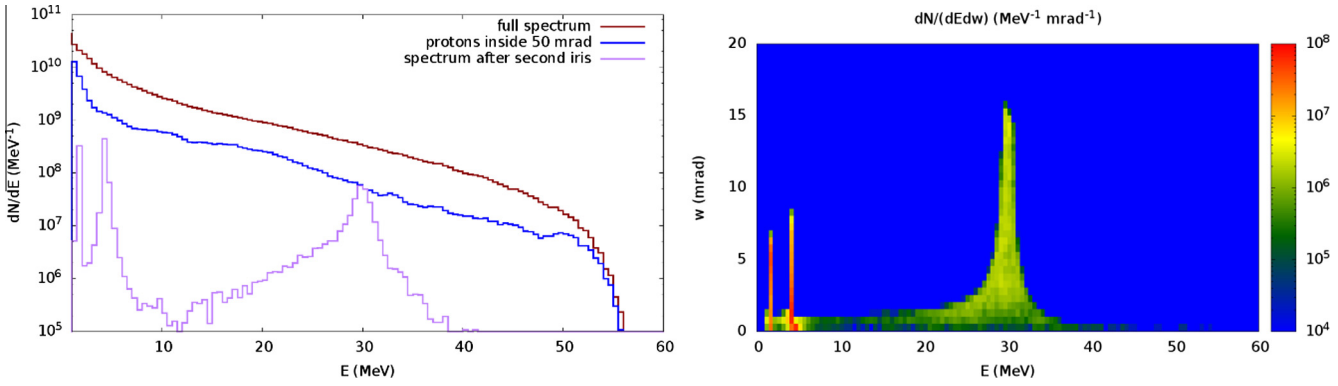

Fig. 6. Left: Proton energy spectra for the triple layer target of thickness $\ell_{foil} = 0.3$ μm (dark red for the initial spectrum, blue after selection at $\theta < 50$ mrad imposed by the first collimator, purple after energy selection operated by the second collimator located on the focal point of the solenoid for the 30 MeV protons). Right: color plot for energy angle spectrum after energy selection. (For interpretation of the references to color in this figure legend, the reader is referred to the web version of this article.)

[16–18]. This was conceived as a side coupled linac designed as a booster for a 30 MeV proton injector working at 3 GHz. Post acceleration with ACLIP allows to obtain a strongly monochromatic bunch at 60 MeV with $\Delta E = 0.1$ MeV and angular spread below 10 mrad with $N \sim 0.5 \times 10^7$ protons. Energy selection with a quadruplet of quadrupoles produced a similar proton bunch before and after post-acceleration but the intensity is lower by one order of magnitude.

In Fig. 7 we show a sketch of the transport line with a solenoid and a quadruplet of permanent magnetic quadrupoles.

4. Conclusions

Preliminary experiments on proton acceleration in the TNSA regime with solid targets are underway at the FLAME facility of the INFN National Laboratory in Frascati. At the present maximum laser intensity of 10^{19} W/cm^2, due to the existing F/10 off-axis parabola, consistently with numerical simulations, a proton beam with maximum energy of few MeV has been measured. Our experimental investigation continues with the challenging goal to make available a laser driven proton test facility to explore acceleration process control, reproducibility and stability, and post acceleration techniques. When the laser intensity on target will be upgraded to $I \approx 10^{21}$ W/cm^2, our simulations predict that starting from the full distribution of accelerated protons we might select protons with $E = 30$ MeV and a narrow spread ΔE and still have a reasonable number of protons (10^7 – 10^8). This opens a very interesting perspective for applications such as hadron therapy, in connection with a post-acceleration stage in order to reach energies up to 60 MeV and beyond using another stage such as the linac booster. Indeed, if a sufficient current intensity can be reached at 30 MeV with a narrow spread $\Delta E/E \sim 1\%$ and a good beam quality after transport, energy selection and collimation, the protons bunch might be post-accelerated after injection in a high field linac, as the one developed for the INFN ACLIP project (suitable for medical applications).

References

[1] H. Daido, M. Nishiuchi, A. S. Pirozhkov, Review of laser-driven ion sources and their applications, Reports on Progress in Physics 75(5) (2012) 056401.
[2] L. Romagnani et al., Laser Part. Beams 26 (2008) 241.
[3] T. Bartal et al., Nat. Phys. 8 (2012) 139.
[4] M. Borghesi, J. Fuchs, S.V. Bulanov, A.J. Mackinnon, P.K. Patel, M. Roth, Fast ion generation by high-intensity laser irradiation of solid targets and applications, Fus. Sci. Technol. 49 (2006) 412.
[5] K. Ogura et al., Opt. Lett. 37 (2012) 2868–2870.
[6] A. Macchi, M. Borghesi, M. Passoni, Rev. Mod. Phys. 85 (2013) 751–793.
[7] M. Passoni, M. Lontano, One-dimensional model of the electrostatic ion acceleration in the ultraintense laser-solid interaction, Laser Part. Beams 22 (2004) 163–169.
[8] K. Zeil, S.D. Kraft, S. Bock, M. Bussmann, T.E. Cowan, T. Kluge, J. Metzkes, T. Richter, R. Sauerbrey, U. Schramm, The scaling of proton energies in ultrashort pulse laser plasma acceleration, New J. Phys. 12 (2010) 045015.
[9] T. Esirkepov, M. Yamagiwa, T. Tajima, Phys. Rev. Lett. 96 (2006) 105001.
[10] C. Benedetti, A. Sgattoni, G. Turchetti, P. Londrillo, ALaDyn: a high-accuracy PIC code for the Maxwell–Vlasov equations, IEEE Trans. Plasma Sci. 36(4) (2008).
[11] L.A. Gizzi et al., NIM B 309 (2013) 202–209.
[12] James F. Ziegler, M. D. Ziegler, J. P. Biersack. SRIM – the stopping and range of ions in matter. Nucl. Instrum. Methods Phys. Res. B 268 (2010) 1818–1823.
[13] T. Burris-Mog, K. Harres, F. Nürnberg, S. Busold, M. Bussmann, O. Deppert, G. Hoffmeister, M. Joost, M. Sobiella, A. Tauschwitz, B. Zielbauer, V. Bagnoud, T. Herrmannsdoerfer, M. Roth, and T. E. Cowan, Phys. Rev. Special Top. Accelerat. Beams 14 (2011) 121301.
[14] S. Sinigardi, G. Turchetti, P. Londrillo, F. Rossi, D. Giove, C. De Martinis, Phys. Rev. Special Top. Accelerat. Beams 16 (2013) 031301.
[15] S. Sinigardi, G. Turchetti, F. Rossi, P. Londrillo, D. Giove, C. De Martinis, P.R. Bolton, "High quality proton beams from a hybrid integrated laser-driven ion acceleration system" Presented at the EAAC workshop 2013 and to be published on NIM A (2013).
[16] V.G. Vaccaro, M.R. Masullo, C. De Martinis, L. Gini, D. Giove, A. Rainò, V. Variale, L. Calabretta, A. Rovelli, S. Barone, Proceedings of the 25th International Linear Accelerator Conference LINAC2010, Tsukuba, Japan (KEK, Tsukuba, Japan, 2010), pp. 467–469.
[17] U. Amaldi, P. Berra, K. Crandall, D. Toet, M. Weiss, R. Zennaro, E. Rosso, B. Szeless, M. Vretenar, C. Cicardi, C. De Martinis, D. Giove, D. Davino, M.R. Masullo, V. Vaccaro, Nucl. Instrum. Methods Phys. Res. Sect. A 521 (2004) 512.
[18] C. De Martinis, D. Giove, U. Amaldi, P. Berra, K. Crandall, M. Mauri, M. Weiss, R. Zennaro, E. Rosso, B. Szeless et al., Nucl. Instrum. Methods Phys. Res. Sect. A 681 (2012) 10.